

Unusual Mechanistic Pathways and Dynamic Processes during Cation Exchange between Substituted Crown Ether–Sodium Complexes in Homogeneous Solution

Yi Li and Luis Echegoyen*

Contribution from the Department of Chemistry, University of Miami, Coral Gables, Florida 33124

Received January 18, 1994*

Abstract: The Na⁺ complexes of 12 substituted aza-crown ethers, some containing amide and others containing ester functional groups as sidearms, were analyzed using dynamic ¹H NMR spectroscopy in CD₃CN solution. For the first time the kinetic activation parameters for cation dissociation from the complexes in the case of the 18-C-6 derivatives were measured. These had failed before when using dynamic ²³Na NMR spectroscopy. An interesting exchange mechanism of the cation directly between two ligand molecules was found to predominate for the ligands that contain a tertiary amide substituent, and to a lesser extent an ester group, but not so if the sidearm contains a secondary amide. Such a mechanistic pathway may be important in cation solvation and stabilization within membrane environments. Additional kinetic processes (besides cation exchange) were “frozen” for these complexes at lower temperatures. These have been attributed to macrocycle inversion at nitrogen, which seems to be hindered and thus thermally accessible after formation of the cation–ligand complexes. The two processes, cation exchange and nitrogen inversion, were successfully resolved in some cases, and the kinetic parameters determined independently. Interestingly, for the 15-C-5 derivatives it was found that the two processes have nearly identical activation parameters, indicating that they are probably coupled.

Introduction

We have recently reported the cation transport rates induced by the presence of lipophilic crown ether derivatives across liposomal membranes.¹ These studies were conducted using ²³Na NMR techniques² in conjunction with aqueous shift reagents to differentiate the intra- and extravascular environments.^{1,3} It was found that several of the substituted crown ether derivative complexes were as efficient cation transporters as some naturally-occurring ionophoric substances such as monensin under identical experimental conditions.^{1,4} These results are not only interesting but also potentially important in the design of synthetic antibiotic agents whose properties effectively simulate those of the traditionally more efficient natural substances.

An important conclusion of this report¹ was the fact that, although the overall Na⁺ transport rate was comparable for the natural and for the synthetic ionophores, their mechanisms differed.¹ While the overall transport process is typically found to be controlled by dissociation of the ionophore–cation complex at the releasing membrane–water interface for the naturally-occurring anionic ionophores, it was found that diffusion of the complex across the membrane environment was rate determining in the case of the synthetic systems.¹ Such fundamental differences are important to understand and to improve the design of substances that some day may even surpass the efficiency of naturally-occurring ones to transport cations across real lipid bilayer membranes. The main reason for the observed mechanistic difference is the presence of a negative charge in the natural antibiotics tested, which is absent in the substituted crown ether compounds.

In order to understand the mechanistic details involved in these cation transporting systems, we recently initiated and reported some homogeneous solution kinetic exchange parameters for these same lipophilic crown ether derivatives using dynamic ²³Na NMR spectroscopy.⁵ It was found that the 18-C-6 derivatives exchange Na⁺ with the solvent primarily via a bimolecular or associative mechanism, while the 15-C-5 ligands prefer a unimolecular or dissociative pathway.^{5,6} It was also concluded in this work that the presence of donor-containing sidearms in the 18-C-6 systems favors the bimolecular mechanism.⁵ Curiously, the 15-C-5 derivatives that contain tertiary amide substituents form unusually inert complexes with Na⁺. Although these complexes are generally less thermodynamically stable than the corresponding 18-C-6 analogues, they are kinetically more stable. All of these interesting conclusions accentuate the importance of knowing the mechanistic and structural details of these complexes both in homogeneous and in heterogeneous (membrane) solutions.

However, using ²³Na NMR spectroscopy it was not possible to obtain activation energies for the cation exchange processes for most of the 18-C-6 derivatives that were investigated.⁵ The reason is that the chemical shifts for solvated and for complexed Na⁺ species are in many cases either too close or one of these is too broad to allow a reasonably accurate determination of the activation parameters. The work presented here uses dynamic ¹H NMR to obtain these parameters. It is also used to probe the possibility of an unusual “associative” mechanism involving two ligand molecules and one Na⁺. The usual associative mechanism for these crown ether complexes involves two cations and one ligand molecule. The unusual associative case, if present, could have significant implications in the process of cation stabilization within membrane environments. While such reactions are not expected to be important for cation binding and stabilization at the membrane–water interface, where cation concentrations are very high, they could be important within the membrane, especially if the transporting ligand system is in the neutral state. Since

* Abstract published in *Advance ACS Abstracts*, July 1, 1994.
(1) Xie, Q.; Li, Y.; Gokel, W. G.; Hernández, J.; Echegoyen, L. *J. Am. Chem. Soc.* 1994, 116, 690.
(2) (a) Buster, D. C.; Hinton, J. F.; Millett, F. S.; Shungu, D. C. *Biophys. J.* 1988, 53, 145. (b) Hills, B. P.; Belton, P. S. *NMR Studies of Membrane Transport*. In *Annual Reports on NMR Spectroscopy*; 1989; Vol. 21, p 100.
(3) Gupta, R. K.; Gupta, P. J. *Magn. Reson.* 1982, 47, 344.
(4) (a) Riddell, F. G.; Hayer, M. K. *Biochim. Biophys. Acta* 1985, 817, 313. (b) Riddell, F. G.; Arumugam, S.; Cox, B. G. *J. Chem. Soc., Chem. Commun.* 1987, 1890. (c) Riddell, F. G.; Arumugam, S. *Biochim. Biophys. Acta* 1988, 945, 65.

(5) Li, Y.; Gokel, W. G.; Hernández, J.; Echegoyen, L. *J. Am. Chem. Soc.* 1994, 116, 3087.

(6) (a) Graves, H. P.; Detellier, C. *J. Am. Chem. Soc.* 1988, 110, 6019. (b) Briere, K. M.; Detellier, C. *New J. Chem.* 1989, 13, 145.

neutrality is typical for many of these crown ether derivatives and desirable for other reasons, these reactions are potentially very important.

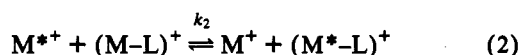
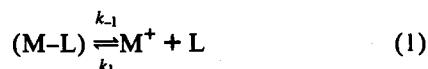
Interestingly, the use of ^1H NMR spectroscopy with these complexes also uncovered the presence of another process that was "frozen" at low temperatures, distinct from the cation exchange reaction. Such a process is present in all of the complexes investigated and is tentatively assigned to macrocyclic nitrogen inversion.

Description of the Model and the Equations

The work presented here owes much to the pioneering efforts of many others who helped establish the NMR techniques to probe the mechanistic details of crown ether complex kinetics.⁷⁻¹⁰ Most notably are the work of Schori et al.,⁷ that of Popov and Dye et al.,^{8,9} and more recently that of Detellier et al.¹⁰ We have recently referenced and described the work from these authors along with the equations that they developed to analyze ^{23}Na NMR results with crown ether-cation complexes.⁵ Therefore, a detailed account of the model and the equations will not be repeated here.

However, since the present work involves the exploration of a novel mechanistic analysis, but one that is conceptually related to previous ones, a brief summary of these prior reactions and equations is presented next. We use equations that look more like those of Popov et al. but follow the conventions of Detellier et al. more closely.⁸⁻¹³

There are two basic mechanisms that together have been invoked to account for all of the alkali metal NMR observations related to the dissociation of crown ether(L)-cation complexes.⁷ These mechanisms, defined as dissociative and associative, can be represented by eqs 1 and 2 below, respectively. In the former, the crown ether-cation complex dissociates mainly by a



unimolecular process as depicted in eq 1. In the other mechanism, an incoming cation (M^{*+} in the equation) interacts with the complex and displaces the bound cation. This mechanism involves the formation of a 1:2 L-(M^+)₂ complex as the transition state. The latter mechanism is favored at high M^+ concentration but depends markedly on the nature of the solvent and the structure of the ligand.⁵ It is possible to determine the relative contributions of these two mechanisms using variable concentration experiments involving alkali metal NMR spectroscopy.^{5,9,13}

Since complexation reactions between crown ethers and cations are generally diffusion controlled^{14,15} association reactions are

(7) Shchori, E.; Jagur-Grodzinski, J.; Luz, Z.; Shporer, M. *J. Am. Chem. Soc.* **1971**, *93*, 7133.

(8) (a) Dye, J. L.; Andrews, C. W.; Ceraso, J. M. *J. Phys. Chem.* **1975**, *79*, 3076. (b) Philips, R. C.; Khazaali, S.; Dye, J. L. *J. Phys. Chem.* **1985**, *89*, 600. (c) Dye, J. L. *Prog. Macrocyclic Chem.* **1979**, *1*, 63.

(9) (a) Lin, J. D.; Popov, A. I. *J. Am. Chem. Soc.* **1981**, *103*, 3773. (b) Schmidt, E.; Popov, A. I. *J. Am. Chem. Soc.* **1983**, *105*, 1873. (c) Szczygiel, P.; Shamsipur, M.; Hallenga, K.; Popov, A. I. *J. Phys. Chem.* **1987**, *91*, 1252. (d) Strasser, B. O.; Hallenga, K.; Popov, A. I. *J. Am. Chem. Soc.* **1985**, *107*, 789. (e) Strasser, B. O.; Popov, A. I. *J. Am. Chem. Soc.* **1985**, *107*, 7921.

(10) (a) Briere, K. M.; Detellier, C. *J. Phys. Chem.* **1987**, *91*, 6097. (b) Briere, K. M.; Detellier, C. *J. Phys. Chem.* **1992**, *96*, 2185. (c) Stover, H. D. H.; Detellier, C. *J. Phys. Chem.* **1989**, *93*, 3174.

(11) Delville, A.; Stover, H. D. H.; Detellier, C. *J. Am. Chem. Soc.* **1985**, *107*, 4172.

(12) Shamsipur, M.; Popov, A. I. *J. Phys. Chem.* **1988**, *92*, 147.

(13) (a) Detellier, C.; Graves, H. P.; Briere, K. M. *Isotopes in the Physical and Biomedical Science*; Elsevier Sci. Publ.: Amsterdam, 1991; Chapter 4. (b) Detellier, C. *Modern NMR Techniques and Their Application in Chemistry*; Popov, A. I., Hallenga, K., Eds.; Marcel Dekker, Inc.: New York, 1990; Chapter 9.

(14) Bouquant, J.; Delville, A.; Grandjean, J.; Laszlo, P. *J. Am. Chem. Soc.* **1982**, *104*, 686.

too fast to be detected directly by NMR spectroscopy. However, the average lifetime of solvated M^+ , τ_A , if modulated by the occurrence of reactions 1 and 2, is given by eq 3. It is also possible to define the average lifetime between the two Na^+ sites

$$\frac{1}{\tau_A [\text{M}^+]_{\text{complex}}} = \frac{k_{-1}}{[\text{M}^+]_{\text{free}}} + k_2 \quad (3)$$

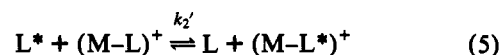
A and B, where B refers to the complex and A is the solvated site, as τ . Since $1/\tau = 1/\tau_A + 1/\tau_B$, it is possible to derive eq 4. This equation has the same form as eq 3 but is expressed in

$$\frac{1}{\tau [\text{M}^+]_{\text{total}}} = \frac{k_{-1}}{[\text{M}^+]_{\text{free}}} + k_2 \quad (4)$$

terms of τ instead of τ_A and $[\text{M}^+]_{\text{total}}$ instead of $[\text{M}^+]_{\text{complex}}$.

Since most crown ether ligands have relatively high binding constants in homogeneous media ($K_S > 10^3 \text{ M}^{-1}$), it is possible to inhibit the associative reaction, eq 2, by simply adjusting the $\text{M}^+:\text{L}$ ratio to 1.0. Under those conditions there is very little free $[\text{M}^+]$, and the reaction is disfavored. However, since the dynamic ^{23}Na NMR method used in our previous work relies in measuring the line width of the solvated $[\text{M}^+]$ signal under slow exchange conditions,⁵ measurements are typically conducted for solutions that contain a $\text{M}^+:\text{L}$ ratio of 2.0. Under those conditions both the associative and dissociative mechanisms compete effectively toward the overall kinetic exchange process of the ligand complexes.

Since dynamic ^{23}Na NMR was not the tool used in the present study, it was not necessary to restrict the measurements to solutions with such stoichiometric proportions. This opened the possibility of exploring the reverse stoichiometric situation, that is, an excess of ligand. Such a situation more realistically represents what goes on inside a membrane phase during the process of cation transportation. The relative saturation of the carrier molecules with cations within the membrane phase is typically low.¹⁶ It is thus interesting to probe the question of whether it is energetically feasible to have an associative cation exchange mechanism, where the cation exchanges directly between two ligand molecules. This situation can be represented by eq 5.



To our knowledge, distinguishing the bimolecular associative mechanism described by eq 5 from the unimolecular process, which is independent of the solution stoichiometry, has not been explored before using NMR spectroscopy. The few reports related to cation exchange of crown ether-cation complexes investigated either via ^1H or ^{13}C NMR have all proposed mechanisms based on multiple assumptions.¹⁷ None of these have presented a treatment as that described here.

It is not difficult to prove that if the two mechanisms that are responsible for cation exchange are those represented by eqs 1 and 5, but not 2, the resulting expression based on τ is given by eq 6. This expression is identical to eq 4, where M^+ was replaced with L and k_2 with k_2' .

$$\frac{1}{\tau [\text{L}]_{\text{total}}} = \frac{k_{-1}}{[\text{L}]_{\text{free}}} + k_2' \quad (6)$$

It is important to recognize that τ refers to the average lifetime of the ligand, which is exchanging between two different states (bound and free) via two different mechanisms. These parameters, although measured for the ligand, reflect the processes

(15) Chock, P. B. *Proc. Natl. Acad. Sci. U.S.A.* **1979**, *69*, 1939.

(16) Fyles, T. M. *Biomimetic Ion Transport with Synthetic Transporters. In Bioorganic Chemistry Frontiers*; Dugas, H., Ed.; Springer-Verlag: Berlin, 1990; Vol. 1, p 71.

(17) (a) Wong, K. H.; Konizer, G.; Smid, J. *J. Am. Chem. Soc.* **1970**, *92*, 666. (b) Lehn, J. M.; Sauvage, J.-P.; Dietrich, B. *J. Am. Chem. Soc.* **1970**, *92*, 2916.

associated with cation exchange. It was possible in most cases to detect a specific ^1H resonance for the ligand in the complex that had a time resolved and different chemical shift from that arising from the same proton in the free ligand, *vide infra*. Thus the kinetics were measured in the slow exchange regime, below the coalescence temperature. For some of our systems, it was necessary to lower the temperature to attain this resolution.

In order to obtain quantitative results for the exchange rates, the Bloch equations modified for chemical exchange must be used to perform a full line shape analysis.¹⁸ This is the most accurate method; however, it contains many pitfalls and is not straightforward. There are several simplified routes for the evaluation of rate constants that are based on line widths or on peak separations as well as on signal intensities or ratios.^{18b} The peak separation method was found to be particularly well suited in the present case, due to the well resolved signals that were observed and the sensitivity of their separation to temperature, *vide infra*. The pertinent equation that was used in the present case was eq 7.¹⁹ In this equation, $\delta\nu_e$ is the observed peak separation and $\delta\nu$ is the separation at

$$k = (\pi/2^{1/2})(\delta\nu^2 - \delta\nu_e^2)^{1/2} \quad (7)$$

extremely slow exchange rates. This expression is valid below and at the coalescence temperature. Care was exercised when applying this equation in the present case, since it is known that if the exchange rates are very slow, $\delta\nu_e$ is not very sensitive and large errors in k may result.

A useful criterion has been derived to evaluate the utility of eq 7 and to ensure that it is properly utilized and that the resulting errors are tolerable.¹⁹ It was shown that the error was within 10% if $\delta\nu/k \leq 5$.^{19b,c} In all of the cases reported here, values were considerably less than 5, typically between 0.5 and 3.0. Although a full line shape analysis might have been more elegant, the relatively large number of systems studied precluded such calculations. This situation, coupled with the fact that the present method was tested for low errors, justified the use of the present treatment.

Based on eq 6, there is a fairly easy way to determine the relative importance of mechanisms 1 and 5.^{5,12,20} With multiplication of eq 6 by $[\text{L}]_{\text{total}}$, eq 8 is obtained. Since the

$$\frac{1}{\tau} = k_{-1} \frac{[\text{L}]_{\text{total}}}{[\text{L}]_{\text{free}}} + k_2' [\text{L}]_{\text{total}} \quad (8)$$

relative ratio of $[\text{L}]_{\text{total}}$ to $[\text{Na}^+]$ was always kept constant at 2, *vide infra*, and since the stability constants for all of the ligands studied are relatively high,^{5,21} $[\text{L}]_{\text{total}}/[\text{L}]_{\text{free}}$ is always the same. Therefore, a dilution experiment, where the total sample concentration is changed progressively, will quickly establish the relative importance of these two mechanisms. If there is a pronounced contribution from reaction 5, then dilution will result in pronounced changes in τ . However, no spectral changes are expected if k_{-1} is dominant.

The quantitative determination of the relative contributions of these two mechanisms requires the construction of plots of $1/\tau$ vs $1/[\text{L}]_{\text{free}}$. From the slope and intercepts it is easy to obtain the values of the exchange rate constants, k_{-1} and k_2' , and thus the relative contributions of these mechanisms.

In addition to variable concentration studies designed to unravel the mechanistic details, variable temperature studies were also

(18) (a) Kaplan, J. I.; Fraenkel, G. *NMR of Chemically Exchanging Systems*; Academic Press: New York, 1980. (b) Sandstrom, J. *Dynamic NMR Spectroscopy*; Academic Press Publishers: New York, 1982.

(19) (a) Gutowsky, H. S.; Holm, C. H. *J. Chem. Phys.* 1956, 25, 1228. (b) Allerhand, A.; Gutowsky, H. S.; Jonas, J.; Meinzer, R. A. *J. Am. Chem. Soc.* 1966, 88, 3185. (c) Oki, M. *Applications of Dynamic NMR Spectroscopy to Organic Chemistry*; VHC Publishers, Inc.: Deerfield Beach, FL, 1985.

(20) Lochhart, J. C.; McDonnell, M. B.; Clegg, W.; Hill, M. N. S.; Todd, M. *J. Chem. Soc., Dalton Trans.* 1989, 203.

(21) Hernandez, J. C.; Trafton, J. E.; Gokel, G. W. *Tetrahedron Lett.* 1991, 6269.

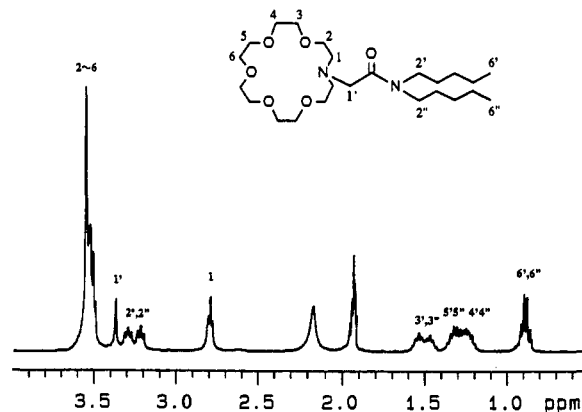
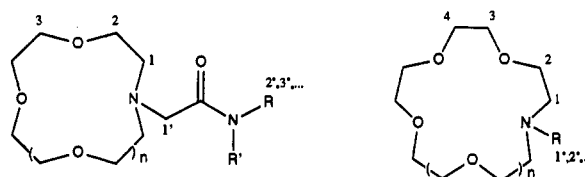


Figure 1. ^1H NMR spectrum of $(18\text{N})\text{CH}_2\text{CON}(\text{C}_5\text{H}_{11})_2$ in CD_3CN .

conducted to determine the values of the activation parameters for the dissociation reactions.

Results and Discussion

General Description of Compounds and ^1H NMR Spectra. As in our previously published work with these ligands,⁵ the same nomenclature is adopted here. The general structures of the compounds are shown below, along with the numbering scheme used to identify different molecular positions. To avoid using



consecutive numerals to identify all of the compounds which is always confusing, the following scheme was adopted to refer to the compounds. The symbol (00N) was used to represent an aza-crown ether having 00 atoms in the macrocoring. The sidearms attached to the macrocoring nitrogen are explicitly written following the ring identifier. There was an additional compound studied here, a diaza-crown, and this is represented as (N18N)[$\text{CH}_2\text{CO-N}(\text{C}_5\text{H}_{11})_2$]₂, indicating that it is a 1,10-diaza-18-C-6, and each macrocoring nitrogen is directly substituted with one dialkyl amide functionality. A total of 12 compounds were investigated; see the results in the tables for specific structures.

A typical 400 MHz ^1H NMR spectrum is presented in Figure 1, along with the specific resonance assignments for $(18\text{N})\text{CH}_2\text{CO-N}(\text{C}_5\text{H}_{11})_2$. All assignments were confirmed by 2D COSY spectra. Of particular interest is the observation of the signal for protons H-1, which appear as an averaged sharp triplet, although it should be more accurately defined as an AA'BB' system, *vide infra*. This resonance is considerably upfield shifted relative to all other macrocoring protons. Such upfield shifts of aza-crown ether systems upon complexation with a metal cation have been previously noted.^{23,24} A rigorous explanation for this phenomenon has not been presented. However, since it has been observed for a wide variety of structural variations, some of which did not contain binding carbonyl groups, it can be safely established that the shift is not exclusively due to the anisotropy of this group. In the present case, the carbonyl is known to interact with the macrocyclic-bound cation.²⁵

All other macrocoring proton resonances have overlapped signals centered around 3.5–3.6 ppm. In addition, this H-1 signal is free

(22) (a) Stewart, W. E.; Siddall, T. H., III *Chem. Rev.* 1970, 70, 517. (b) Whittaker, A. G.; Moore, D. W.; Siegel, S. *J. Phys. Chem.* 1964, 68, 3431.

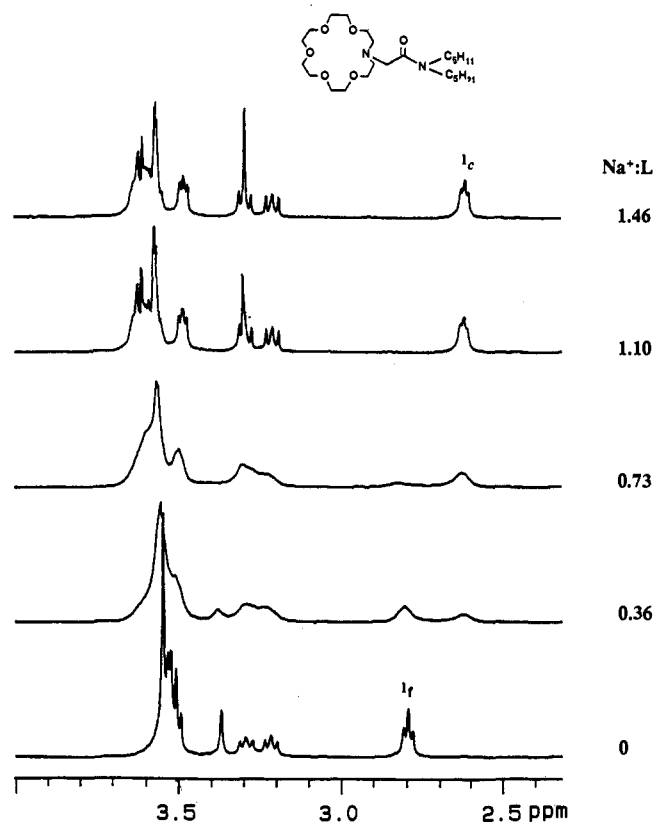
(23) Lehn, J. M.; Simon, J. *Helv. Chim. Acta* 1977, 60, 141.

(24) Graf, E.; Lehn, J. M. *J. Am. Chem. Soc.* 1975, 97, 5022.

(25) Fronczek, F. R.; Gatto, V. J.; Minganti, C.; Schultz, R. A.; Gandour, R. D.; Gokel, G. W. *J. Am. Chem. Soc.* 1984, 106, 7244.

Table 1. ^1H NMR Chemical Shifts (ppm) of Aza-Crown Ether Derivatives in CD_3CN

| compound | proton position | | | | | NH |
|---|-----------------|------|------|------|-------------------|------|
| | 1 | 2 | 1' | 2' | 2'' | |
| (12N) $\text{CH}_2\text{-CO-N}(\text{C}_5\text{H}_{11})_2$ | 2.76 | | 3.32 | 3.22 | 3.33 | |
| (15N) $\text{CH}_2\text{-CO-N}(\text{C}_5\text{H}_{11})_2$ | 2.74 | | 3.33 | 3.22 | 3.29 | |
| (15N) $\text{CH}_2\text{-CO-N}(\text{C}_{10}\text{H}_{21})_2$ | 2.74 | | 3.32 | 3.21 | 3.29 | |
| (15N) $\text{CH}_2\text{-CO-NHC}_5\text{H}_{11}$ | 2.64 | 3.48 | 3.02 | 3.14 | | 7.91 |
| (15N) $\text{CH}_2\text{-CO-NHC}_{10}\text{H}_{21}$ | 2.64 | 3.48 | 3.02 | 3.13 | | 7.91 |
| (15N) $\text{CH}_2\text{-CO-OC}_{10}\text{H}_{21}$ | 2.79 | | 3.38 | 4.04 | | |
| (18N) $\text{CH}_2\text{-CO-N}(\text{C}_6\text{H}_{11})_2$ | 2.79 | | 3.36 | 3.22 | 3.30 | |
| (18N) $\text{CH}_2\text{-CO-N}(\text{C}_{10}\text{H}_{21})_2$ | 2.78 | | 3.34 | 3.21 | 3.29 | |
| (18N) $\text{CH}_2\text{-CO-NHC}_{10}\text{H}_{21}$ | 2.67 | 3.45 | 2.99 | 3.14 | | 7.71 |
| (18N) $\text{CH}_2\text{-CO-NHC}_{18}\text{H}_{37}$ | 2.67 | 3.44 | 2.98 | 3.13 | | 7.71 |
| (18N) $\text{CH}_2\text{-CO-OC}_{10}\text{H}_{21}$ | 2.82 | | 4.03 | | | |
| (N18N) $[\text{CH}_2\text{-CO-N}(\text{C}_5\text{H}_{11})_2]_2$ | 2.77 | | 3.32 | 3.22 | 3.32 ^a | |

^a Estimated value because of signal overlap.**Figure 2.** ^1H NMR spectra of $(18\text{N})\text{CH}_2\text{CON}(\text{C}_5\text{H}_{11})_2$ titrated with NaBPh_4 in CD_3CN . 1_f and 1_c are the H-1 signals of the free and complexed ligands, respectively.

from overlap with any others in the spectrum and, as will be seen shortly, is a good probe of the ligand's binding properties. Not surprisingly the two amide side chains did not exhibit equivalent protons, a reflection of the hindered rotation around the CO-N bond. The specific assignments presented in Figure 1 for the two nonequivalent alkyl chain protons is based on empirical observations made for *N,N*-diethylalkylamide and higher analogues, which assign alkyl protons that are *cis* to the carbonyl oxygen to lower field than those that are *trans*.²² Table 1 shows some of the ^1H NMR chemical shifts of the compounds studied here.

A series of titration experiments were conducted at a constant ligand concentration of 10 mM, varying the $\text{Na}^+:\text{ligand}$ ratio between 0 and 3. As expected, significant spectral changes were observed for the H-1 resonance upon addition of NaBPh_4 . Figure 2 shows the titration results for $(18\text{N})\text{CH}_2\text{CON}(\text{C}_5\text{H}_{11})_2$, conducted at room temperature. It is evident that addition of Na^+ results in the appearance of an additional, time resolved signal for H-1 in the complex and that this resonance, initially broad, dominates the spectrum entirely after one stoichiometric

equivalent of Na^+ has been added. Such an observation clearly indicates that a two-jump model is operative and that the H-1 resonances are a convenient handle to probe ligand-cation binding kinetics.

It was interesting to find out that such simultaneous observation of the H-1 resonances for the free ligand and for the ligand-cation complex were only observed at room temperature for the tertiary amide containing 18-C-6 derivatives and for (N18N)- $[\text{CH}_2\text{CON}(\text{C}_5\text{H}_{11})_2]_2\text{Na}^+$. The secondary amide derivatives, $(18\text{N})\text{CH}_2\text{CONH}(\text{C}_n\text{H}_{2n+1})$, and the ester substituted systems, $(18\text{N})\text{CH}_2\text{COO}(\text{C}_n\text{H}_{2n+1})$, did not show such signal separation when partially complexed by Na^+ . In these cases, only a time averaged signal for H-1 was recorded at room temperature throughout the titration experiment. Fortunately, when the samples were cooled down to -40°C , the H-1 resonances of all of the 18-C-6 systems studied exhibited two resolved signals for the free ligand and for the Na^+ complex. It was therefore possible to watch, in most cases, the transition between a single, coalesced H-1 resonance to separate resonances for the ligand species. This allowed the use of eq 7 to determine the kinetic parameters as described above. There was only one case where it was not possible to observe coalescence of the H-1 resonances even at high temperature. This was the situation with (N18N) $[\text{CH}_2\text{CON}(\text{C}_5\text{H}_{11})_2]_2\text{Na}^+$.

Dilution Experiments. One of the important justifications for the present work was the idea of probing for the existence of mechanism 5, which has not been previously investigated for crown ether-cation complexes. In order to establish if mechanism 5 was operative in these systems, and, if so, to determine the relative importance of the two cation exchange mechanisms, eq 1 and 5, dilution experiments were conducted for several of the ligand- Na^+ systems, always keeping the $\text{L}:\text{Na}^+$ ratio at 2. Figure 3 shows a typical spectral response for tertiary amide and for secondary amide 15-C-5 derivative- Na^+ complexes, and Figure 4 shows the same for a tertiary amide 18-C-6 derivative- Na^+ complex and for (N18N) $[\text{CH}_2\text{CON}(\text{C}_5\text{H}_{11})_2]_2\text{Na}^+$. Notice the pronounced change observed for the H-1 resonances in Figure 3a,b, which goes from a coalesced to a resolved set of signals upon dilution by a factor of 20. This is a clear indication that mechanism 5 must be predominant. To our knowledge this is the first time that such a mechanistic observation has been experimentally confirmed.¹⁷

Similarly, a pronounced concentration dependence of the spectra was observed for the tertiary amide 18-C-6 derivative- Na^+ complexes upon dilution, Figure 4a,b. On the other hand, dilution by the same factor of 20 did not result in any appreciable spectral changes in Figures 3c,d or 4c,d. It is actually possible to make the following generalization; tertiary amide substituted monoaza-crown ethers favor cation exchange via eq 5. Secondary amide cases favor the unimolecular pathway, eq 1. This generalization holds true regardless of the macroring size. The only exception found was the case of the diaza-crown system, which contains tertiary amide substituents but seems to favor complex dissociation via the dissociative mechanism. This point is addressed later.

Of all of the systems investigated, $(18\text{N})\text{CH}_2\text{CON}(\text{C}_{10}\text{H}_{21})_2\text{Na}^+$ is the only one that exhibited clear signal separation in the available concentration range to allow the quantitative separation of the two mechanisms. The overall rates of exchange were calculated using eq 7 for the different total concentrations, and the $1/\tau[\text{L}]_{\text{total}}$ vs $1/[\text{L}]_{\text{free}}$ plot was constructed, Figure 5. From the slope and intercept of this graph the values of k_{-1} and k_2' were calculated to be 6.5 s^{-1} and $2.8 \times 10^3\text{ s}^{-1}\text{ M}^{-1}$, respectively. Although these numbers indicate that the unimolecular pathway is not completely inoperative, the bimolecular mechanism is the major contributor to the overall exchange process. These rate constant values, following the Eyring equation, indicate that the

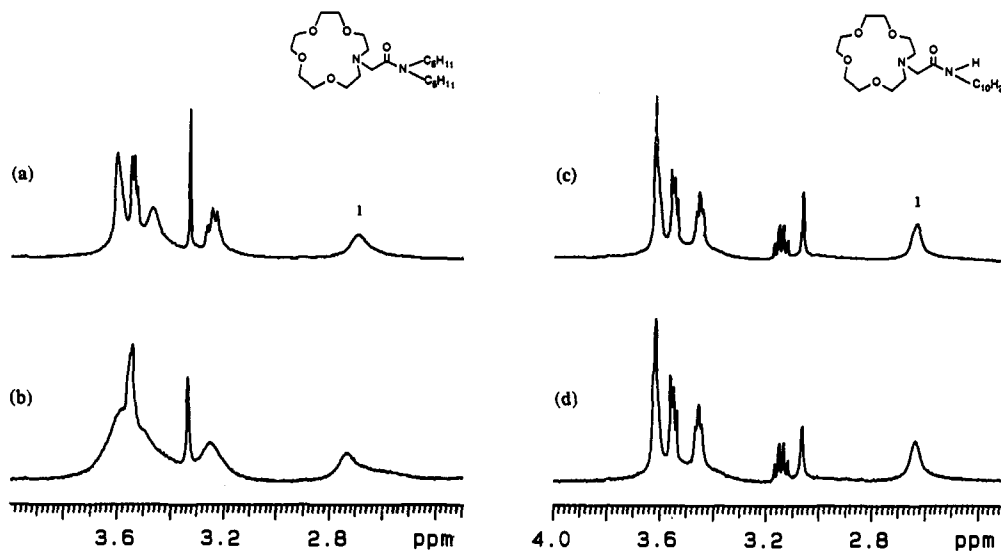


Figure 3. ^1H NMR spectra of $(^{15}\text{N})\text{CH}_2\text{CON}(\text{C}_5\text{H}_{11})_2$ (a,b) and $(^{15}\text{N})\text{CH}_2\text{CONHC}_5\text{H}_{11}$ (c,d) in the presence of NaBPh_4 with $\text{L}:\text{Na}^+$ ratio of 2:1 at (a) 34.3, (b) 1.7, (c) 33.8, and (d) 1.7 mM.

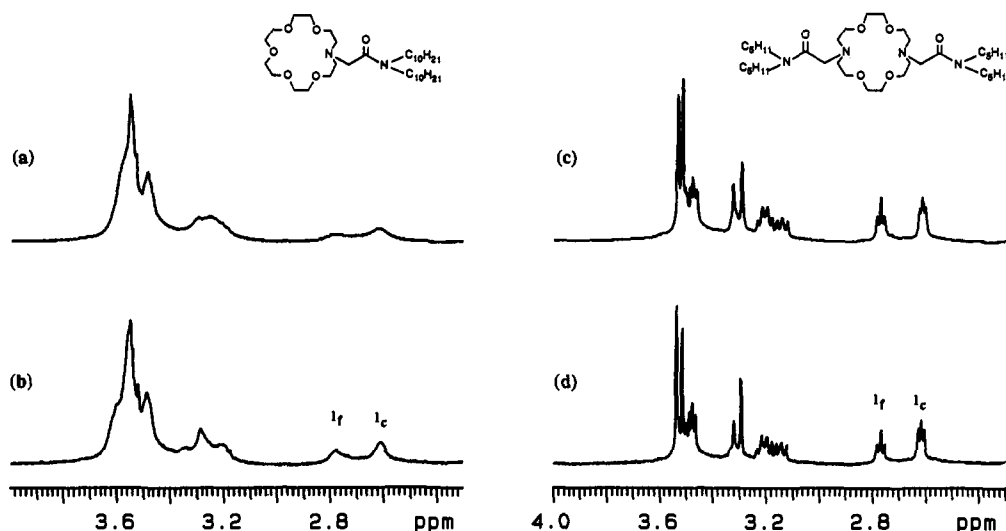


Figure 4. ^1H NMR spectra of $(^{18}\text{N})\text{CH}_2\text{CON}(\text{C}_{10}\text{H}_{21})_2$ (a,b) and $(\text{N}^{18}\text{N})[\text{CH}_2\text{CON}(\text{C}_5\text{H}_{11})_2]_2$ (c,d) in the presence of NaBPh_4 with $\text{L}:\text{Na}^+$ ratio of 2:1 at (a) 18.4, (b) 2.3, (c) 17.9, and (d) 0.9 mM. 1_f and 1_c are the H-1 signals of the free and complexed ligands, respectively.

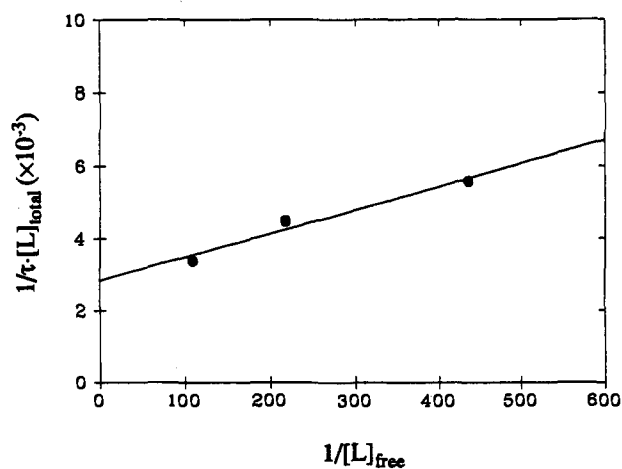


Figure 5. Plot of $1/\tau[\text{L}]_{\text{total}}$ vs $1/[\text{L}]_{\text{free}}$ for the $(^{18}\text{N})\text{CH}_2\text{CON}(\text{C}_{10}\text{H}_{21})_2\text{-Na}^+$ complex in CD_3CN .

bimolecular mechanism has a free energy of activation, $\Delta G^{\ddagger\text{bi}}$, which is 3.5 Kcal/mol lower than $\Delta G^{\ddagger\text{uni}}$, both calculated at 21 $^\circ\text{C}$.

It is interesting to compare the mechanistic observations made here in the presence of excess ligands with those previously reported

for the same ligands in the presence of excess Na^+ .⁵ When there is excess of Na^+ , ^{23}Na NMR results conclusively showed that the bimolecular (eq 2 above, not 5) pathway dominated for 18-C-6 derivatives, while the unimolecular process dominated for the 15-C-5 compounds. Thus, under those conditions, the macroring size seems to be the most important determinant of mechanistic preference. However, under the presently explored conditions, the nature of the sidearm seems to determine the preferred mechanistic pathway. This point is addressed later after the activation parameters are presented.

Variable Temperature Studies and Activation Parameters. As mentioned in the Introduction, part of the impetus for the present ^1H NMR work stemmed from the desire to measure the activation parameters for cation exchange from the 18-C-6 derivative- Na^+ complexes, which had failed using ^{23}Na NMR spectroscopy.⁵ In order to do so, variable temperature experiments were conducted. All experiments were conducted at a 2:1, $\text{L}:\text{Na}^+$ ratio, with $[\text{L}]_{\text{total}} = 10$ mM in CD_3CN . Again, eq 7 was used to determine the kinetic parameters as a function of temperature.

Figure 6 shows a typical dynamic NMR sequence for one of the ligand complexes studied. Notice that the H-1 resonances from the free ligand and from the complex are coalesced at 70 $^\circ\text{C}$ but separate clearly into two approximately equal intensity resonances at lower temperatures. Coalescence for this particular

Table 2. Activation Parameters of the Sodium Exchange Process for 18-C-6 Derivative-Na⁺ Complexes Measured by ¹H NMR in CD₃CN^b

| compound | $\Delta G^{\ddagger}_{21^\circ\text{C}}$, kcal/mol | ΔH^{\ddagger} , kcal/mol | ΔS^{\ddagger} , cal/mol-K | ΔG^{\ddagger}_0 , kcal/mol | T_0 , °C |
|--|---|----------------------------------|-----------------------------------|------------------------------------|------------|
| (18N)CH ₂ -CO-N(C ₅ H ₁₁) ₂ | 14.11 _(0.02) | 0.64 _(0.04) | -45.8 _(0.02) | 15.5 | 48 |
| (18N)CH ₂ -CO-N(C ₁₀ H ₂₁) ₂ | 14.00 _(0.01) | 0.45 _(0.05) | -46.1 _(0.02) | 15.4 | 45 |
| (18N)CH ₂ -CO-NHC ₁₀ H ₂₁ | 14.0 _(0.3) | 4.3 _(0.4) | -33.0 _(0.2) | 13.3 | -5 |
| (18N)CH ₂ -CO-NHC ₁₈ H ₃₇ | 14.10 _(0.02) | 4.1 _(0.2) | -34.0 _(0.6) | 13.5 | -2 |
| (18N)CH ₂ -CO-OC ₁₀ H ₂₁ | 14.03 _(0.07) | 1.7 _(0.1) | -41.8 _(0.1) | 13.8 | 13 |
| (18N)[CH ₂ -CO-N(C ₅ H ₁₁) ₂] ₂ | | | | >16.7 | >70 |
| 18-C-6 | 13.8 ^a | 1.8 ^a | -40.8 ^a | | |
| (18N)(CH ₂) ₃ CH=CH ₂ | 12.6 ^a | 5.1 ^a | -25.6 ^a | | |
| | 13.4 ^a | 4.7 ^a | -29.7 ^a | | |

^a From ²³Na NMR measurement.⁵ ^b The numbers in the parentheses are the standard deviations.

case occurs around 48 °C. Interestingly, the H-1 resonance at higher field, assigned to the complex, broadens below 0 °C, and is very broad at -30 °C. This is not the case for the free ligand H-1 resonance at lower field. This is the onset of another kinetic process being frozen at these extreme low temperatures and is more clearly observed for other systems, *vide infra*.

Of all of the systems studied, it was not possible to induce coalescence for (N18N)[CH₂CON(C₅H₁₁)₂]₂Na⁺, even at the highest temperatures attainable under the present experimental conditions, ~70 °C. This was the only complex for which this was true. Although the H-1 resonances for the free and for the complexed ligand exhibited some broadening at this temperature, they were still well resolved. It was thus only possible to set a lower limit value for ΔG_C^{\ddagger} .

The activation parameters for all of the 18-C-6 derivatives investigated are presented in Table 2. The values for the 15-C-5 derivative complexes and for the 12-C-4 derivative were not determined due to the presence of coexisting dynamic processes at similar temperatures, which precluded their accurate determination. This is not tragic since cation exchange from these smaller ring macrocyclic compounds have already been determined using dynamic ²³Na NMR spectroscopy and reported.⁵ The origin of the interfering processes is the subject of the next section.

The most notable results from Table 2 are the extremely low activation enthalpies found for the tertiary amide derivative azacrown complexes. The two entries in the table are very low, considerably less than 1 kcal/mol. Contrastingly, the two entries in Table 2 corresponding to the secondary amide derivative complexes are larger and similar to each other, around 4 kcal/mol. These differences are in agreement with the previously found mechanistic differences between the tertiary and the secondary amide systems. The tertiary amide systems exchange the cation via a bimolecular pathway involving two ligand molecules and one cation. This novel mechanism has a low activation energy when the sidearms involved are good donors, as is the case of the tertiary amides.

The ester derivative complex, (18N)CH₂COOC₁₀H₂₁Na⁺, has an activation enthalpy close to but slightly higher than that of the tertiary amide cases, probably indicating that the mechanism involved is also bimolecular and that this is favored over the unimolecular dissociative process. The higher activation enthalpy for the ester is probably a reflection of its lower donor ability, relative to the tertiary amide.

The secondary amide cases have activation enthalpies that are very close to those determined for 18-C-6-Na⁺ and (18N)(CH₂)₃-CH=CH₂Na⁺, which have been shown, using dynamic ²³Na NMR spectroscopy to exchange the cation primarily via a unimolecular mechanism.⁵ It is thus safe to assume that the dissociative mechanism predominates in the secondary amide substituted systems.

Based on the structural and electronic properties of these crown ethers, the explanation for these observations is rather straightforward. We recently showed unequivocal 2D NMR evidence that proved that the secondary amide compounds presented here exhibit a high degree of intramolecular hydrogen bonding.¹

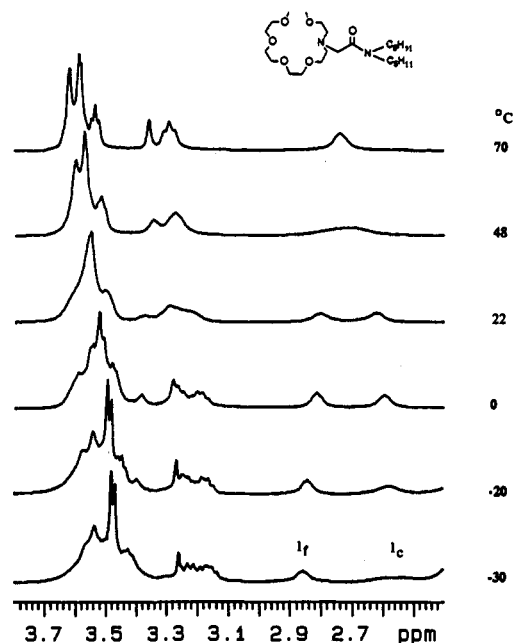


Figure 6. ¹H NMR spectra of (18N)CH₂CON(C₅H₁₁)₂Na⁺ in the presence of NaBPh₄ at a 2:1 L:Na⁺ ratio at various temperatures. 1_f and 1_c are the H-1 signals of the free and complexed ligands, respectively.

Therefore, we believe that the free sidearm in an uncomplexed ligand molecule is able to approach a complexed cation, probably from the side opposite to where the sidearm is interacting with the cation in the complex. Such a process would obviously be favored by high donicity of the sidearm, as for tertiary amides and, to a lesser degree, for the ester. On the other hand, such an approach is inhibited in the case of the secondary amide systems by virtue of the intramolecular H-bond that forms between the amide hydrogen and the macrocycle for the uncomplexed ligand. Therefore, the dissociative mechanism predominates in these cases, and the activation enthalpies are consequently higher.

A case that deserves special mention is that of the diaza-crown system, (N18N)[CH₂CON(C₅H₁₁)₂]₂Na⁺, which must have the largest activation parameters of all of the cases studied. The interpretation of these results are perfectly consistent with the model presented in the previous paragraph if one considers that the two sidearms in a complex block the approach of a free ligand. Therefore, even though the sidearms are tertiary amides and thus expected to favor an associative pathway, the fact that there are two sidearms located in the complex sterically disfavors such an approach. This in turn leads to the formation of what appears to be the most kinetically stable of all of the complexes investigated here.

An interesting point to note is that all of the 18-C-6 derivatives investigated exhibited nearly identical free energies of activation, Table 2. This must be the result of strong enthalpy-entropy compensation effects, as discussed elsewhere.²⁶

(26) Delville, A.; Stover, H. D. H.; Detellier, C. J. *J. Am. Chem. Soc.* 1987, 109, 7293.

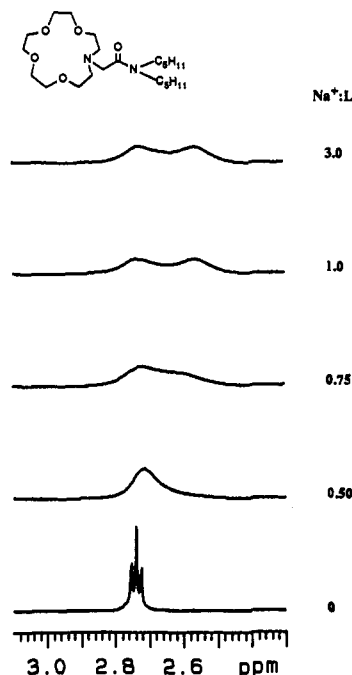


Figure 7. ^1H NMR spectra of $(15\text{N})\text{CH}_2\text{CON}(\text{C}_5\text{H}_{11})_2$ titrated with NaBPh_4 in CD_3CN .

Additional Kinetic Processes in 15-C-5 and 12-C-4 Derivatives.

It has already been mentioned that the 15-C-5 and 12-C-4 derivative complexes in this study exhibit additional kinetic processes that interfere with that of cation exchange. In the case of the 18-C-6 systems, these processes are also present and visible (see, for example, Figure 6 at very low temperatures), but they occur at much lower temperatures than those needed to freeze cation exchange reactions, and therefore they do not interfere.

A clear proof of the existence of such an additional process in one of the 15-C-5 derivatives is presented in Figure 7, which is the titration of $(15\text{N})\text{CH}_2\text{CON}(\text{C}_5\text{H}_{11})_2$ with NaBPh_4 in CD_3CN . The H-1 signal, which starts as the usual sharp triplet for the free ligand, broadens at about a $\text{L}:\text{Na}^+$ ratio of 2. This broadening must be the result of cation exchange. Interestingly, as the ratio approaches unity, the signal splits into two broad resonances of approximately equal intensity. Even if the $\text{L}:\text{Na}^+$ ratio is further decreased to 1/3, the signal remains the same. Notice how this behavior contrasts that observed in Figure 2, where the H-1 signal that was present after the addition of one stoichiometric equivalent of Na^+ and beyond was that of a single species, the complex. Since the K_S value for $(15\text{N})\text{CH}_2\text{CON}(\text{C}_5\text{H}_{11})_2$ with Na^+ is large,²¹ the signal observed after 1 equiv of Na^+ is added must correspond exclusively to that of the complex. The conclusion must therefore be that the broad H-1 resonances observed reflect a slow intramolecular process taking place within the complex. Such a slow process must be due to a relatively rigid molecular structure brought about by the complexation with the cation.

In order to find further confirmation for this behavior and support for its interpretation, the same ligand was titrated with CaClO_4 . Since Ca^{2+} has a similar ionic radius to Na^+ and since it is doubly charged, it was anticipated that it would result in an even more rigid molecular structure after complexation. Indeed the H-1 signal of all of the Ca^{2+} complexes are split into two, each one of which is composed of eight very sharp signals. Eight is the number expected for splitting from three nonequivalent neighbors, which are the other H-1 proton and the two H-2 hydrogens. Therefore, it is clear that the 1:1 complexes with Ca^{2+} also have a very rigid structure and that there is an additional intramolecular kinetic process that is now frozen at room temperature.

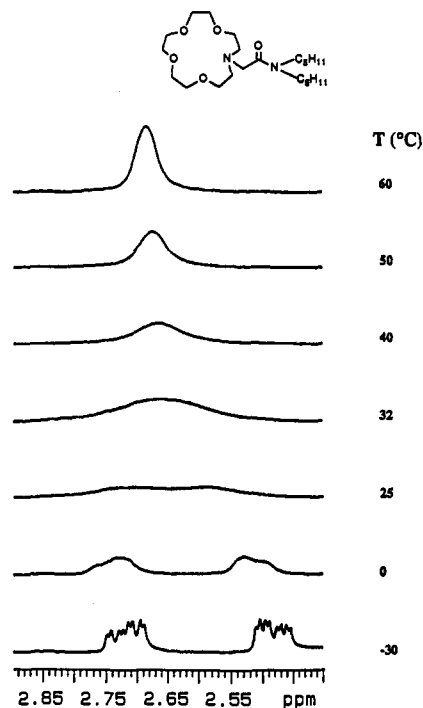


Figure 8. ^1H NMR spectra of $(15\text{N})\text{CH}_2\text{CON}(\text{C}_5\text{H}_{11})_2\text{Na}^+$ complex in CD_3CN at a 1:1 $\text{L}:\text{Na}^+$ ratio at various temperatures.

The variable temperature behavior of these complexes was probed, and that for the $(15\text{N})\text{CH}_2\text{CON}(\text{C}_5\text{H}_{11})_2\text{Na}^+$ complex, at a 1:1 relative ratio, is shown in Figure 8. It must be stressed that the H-1 signal arises exclusively from the 1:1 complex, and thus any changes must reflect intramolecular processes and not intermolecular cation exchange reactions, as in previous figures. Notice that at 60 °C, the intramolecular process has coalesced, and only a single signal is observed. As the temperature is lowered, the process slows down until it is frozen, and this is clearly visible at 0 °C. Further cooling to -30 °C results in the appearance of a spectrum for H-1 that is very similar to that observed for the corresponding Ca^{2+} complex at room temperature. Thus the dynamic processes involved in these two complexes must be similar. An important point that needs to be made is that no NMR spectral changes were observed within the full temperature range available in these experiments for most of the free ligands investigated here. ^1H NMR spectra remained essentially identical for these between 70 and -40 °C. Only $(12\text{N})\text{CH}_2\text{CON}(\text{C}_5\text{H}_{11})_2$ exhibited some broadening at -40 °C, since, due to its smaller ring size, intramolecular motions are somewhat more restricted, *vide infra*.

The nature of the additional kinetic processes observed for the complexes, distinctly different from that for the cation exchange reaction, can be guessed from comparisons with the results for acyclic and cyclic trialkyl amines.²⁷ These systems exhibit both nitrogen inversion and $\text{CH}_2\text{-N}$ rotational barriers that can be frozen in some cases. While the rotational barriers are too low for the acyclic molecules to be observable by NMR spectroscopy, nitrogen inversion is typically accessible.^{27,28} In the cyclic molecules, even the $\text{CH}_2\text{-N}$ rotational barriers are sufficiently increased due to internal rigidity that they also become accessible by NMR spectroscopy.²⁹

We thus propose that the process being frozen at about 25 °C in Figure 8, clearly visible at 0 °C, corresponds to restricted nitrogen inversion of the complex. The additional sharpening of the signals observed between 0 and -30 °C could be due to freezing

(27) Lambert, J. B.; Takeuchi, Y. *Acyclic Organonitrogen Stereodynamics*; Marchand, A. P., Ed.; VCH Publishers, Inc.: New York, 1992.

(28) Fleischman, S. H.; Whalon, M. R.; Rithner, C. D.; Grady, G. L.; Bushweller, C. H. *Tetrahedron Lett.* 1982, 4233.

(29) Gutowsky, H. S.; Temussi, P. A. *J. Am. Chem. Soc.* 1967, 89, 4358.

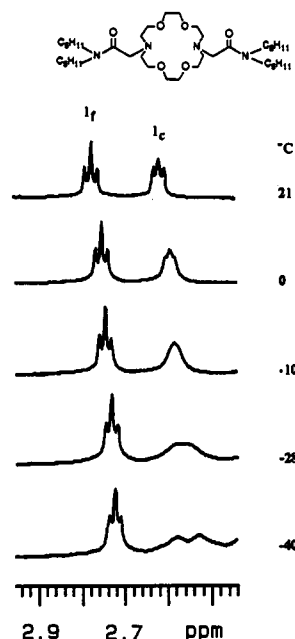


Figure 9. ^1H NMR spectra of $(\text{N18N})[\text{CH}_2\text{CON}(\text{C}_5\text{H}_{11})_2]_2$ in the presence of NaBPh_4 at a 2:1 $\text{L}:\text{Na}^+$ ratio at various temperatures. 1_f and 1_c are the H-1 signals of the free and complexed ligands, respectively.

of some $\text{CH}_2\text{-N}$ rotational processes. The latter assignment is more uncertain but is in line with similar observations and interpretations for amine compounds.²⁷⁻²⁹

Separation and Quantification of Coexisting Kinetic Processes. Because of severe signal overlap for the free ligand and the complex in the cases of the 15-C-5 and 12-C-4 derivatives (see Figure 7 for examples), it was impossible to monitor selectively and quantitatively the spectral changes due to complex dissociation and those due to other processes, such as nitrogen inversion. An additional complication was the fact that both cation exchange and nitrogen inversion coalesce at similar temperatures for these smaller macrocyclic ligands. It was thus necessary to begin with the 18-C-6 series to monitor these changes within the same sample.

The most obvious starting point was to select one of the systems where the cation exchange process is frozen, even at room temperature. These systems include $(18\text{N})\text{CH}_2\text{CON}(\text{C}_5\text{H}_{11})_2\text{Na}^+$, $(18\text{N})\text{CH}_2\text{CON}(\text{C}_{10}\text{H}_{21})_2\text{Na}^+$, and $(\text{N18N})[\text{CH}_2\text{CON}(\text{C}_5\text{H}_{11})_2]_2\text{Na}^+$, all at a $\text{L}:\text{Na}^+$ ratio of 2. Results for the first case were already presented in Figure 6, but the latter was initially chosen and its variable temperature results are presented in Figure 9 due to its spectral clarity.

At 21 °C, the two H-1 resonances corresponding to the free ligand (at lower field) and to the complex (at higher field) are observed as fairly sharp triplets, Figure 9. As the temperature is lowered, only the H-1 resonance of the complex broadens until, at -40 °C, it is clearly split into two broad resonances. All along, the H-1 signal for the free ligand remains essentially unperturbed. The behavior exhibited by the complex is similar to that shown in Figure 8 for $(15\text{N})\text{CH}_2\text{CON}(\text{C}_5\text{H}_{11})_2\text{Na}^+$, except that the present case coalesces at a much more negative temperature. The process is thus assigned to freezing of the nitrogen inversion process, which is clearly separated unequivocally from the cation exchange reaction.

As mentioned already, Figure 6 also contains a similar example, where the spectrum at 70 °C shows a single line for the coalesced resonance from all kinetic processes. The cation exchange reaction is frozen below 48 °C. Then the nitrogen inversion begins to slow down and broaden the resonance for the complex selectively below 0 °C and is almost seen to yield two very broad resonances at -30 °C.

The coalescence temperature values for the different processes for these systems was as follows. For cation exchange, >70, 48,

and 45 °C, for $(\text{N18N})[\text{CH}_2\text{CON}(\text{C}_5\text{H}_{11})_2]_2\text{Na}^+$, $(18\text{N})\text{CH}_2\text{CON}(\text{C}_5\text{H}_{11})_2\text{Na}^+$, and $(18\text{N})\text{CH}_2\text{CON}(\text{C}_{10}\text{H}_{21})_2\text{Na}^+$, respectively. The respective values for nitrogen inversion were -28, -28, and -26 °C.

For the other 18-C-6 derivative complexes only the cation exchange reaction was frozen at the lowest available temperatures. Although signal broadening of the complexes is evident at -40 °C, no coalescence was achieved for the nitrogen inversion process.

In order to be able to extract quantitative kinetic data for nitrogen inversion for the 15-C-5 and for the 12-C-4 derivatives it was necessary to do the variable temperature experiments on samples containing a 1:1 ratio of $\text{L}:\text{Na}^+$. This eliminated the interference from the cation exchange reaction by totally inhibiting its occurrence. Thus measurements were made for spectra similar to those shown in Figure 8 and the kinetic parameters calculated with the use of eq 7.

A summary of the activation parameters for intraligand motion is provided in Table 3. Notice that for the 18-C-6 derivative series it was only possible to determine the coalescence temperature for nitrogen inversion and thus only $\Delta G^\ddagger_{\text{C}}$ is available. Since T_{C} 's in these cases are very low, it was not possible to do a complete variable temperature study below them. However, it was possible in this series to determine the T_{C} 's for the nitrogen inversion process both at a $\text{L}:\text{Na}^+$ ratio of 1 and 2. Results were identical in all cases, indicating that cation exchange does not interfere with the nitrogen inversion process.

As expected, the activation free energies are lower for the 18-C-6 derivative series than for the smaller ring macrocyclic analogues. This is simply a reflection of the more flexible nature of the 18-C-6 derivative complexes, compared with the smaller macrocycles. Comparing these values to those found for the cation exchange reaction, Table 2, it is clear that these two processes are independent of each other. However, this is not the case for the 15-C-5 and 12-C-4 derivatives.

The $\Delta G^\ddagger_{21^\circ\text{C}}$ values for the nitrogen inversion process for the 15-C-5 and 12-C-4 derivative complexes with Na^+ are very close to those previously determined and reported for their corresponding cation exchange reaction.⁵ Thus these two processes, cation exchange and nitrogen inversion, appear to be coupled. This situation, which contrasts that of the 18-C-6 analogues, is easy to understand from a structural point of view. Complexation of the smaller macrocyclic sizes leads to an increased overall rigidity, comparably speaking with the 18-C-6 series, that in turn results in closer coupling of intramolecular motions. Thus, while the 18-C-6 derivative complexes can retain a higher degree of conformational mobility and thus provide alternative optimal solvation conformations for the cation, the smaller ring systems are not able to do so. Therefore, intramolecular reorganizations are more likely to be coupled in the smaller ring systems. Such a rationalization is also perfectly in accord with the previous finding that 15-C-5 derivative complexes prefer to exchange their cation with the solvent via a dissociative, versus associative, pathway.

Conclusions

A series of 12 lipophilic aza-crown ether- Na^+ complexes were investigated using dynamic ^1H NMR spectroscopy. Their homogeneous cation exchange reactions were studied in CD_3CN as well as other intramolecular kinetic processes which were assigned to restricted nitrogen inversion within the complexes. It was possible for the first time to obtain the activation parameters for cation exchange from the 18-C-6 derivative complexes, which was not possible using dynamic ^{23}Na NMR spectroscopy.

An interesting new mechanistic route was investigated for the cation exchange reaction of these ligands. This route, involving direct cation exchange between two ligands in solution, was found to predominate in the case of ligands containing tertiary amide substituents. Such a finding may have important implications,

Table 3. Activation Parameters of the Nitrogen Inversion Process for Aza-Crown Ether Derivative-Na⁺ Complexes Measured by ¹H NMR^a

| compound | $\Delta G^{\ddagger}_{21^{\circ}\text{C}}$, kcal/mol | ΔH^{\ddagger} , kcal/mol | ΔS^{\ddagger} , cal/mol·K | $\Delta G^{\ddagger}_{\text{c}}$, kcal/mol | T_{c} , °C |
|--|---|----------------------------------|-----------------------------------|---|---------------------|
| (12N)CH ₂ -CO-N(C ₅ H ₁₁) ₂ | 13.9 _(0.1) | 4.8 _(0.4) | -31 ₍₁₎ | 14.0 | 25 |
| (15N)CH ₂ -CO-N(C ₅ H ₁₁) ₂ | 14.2 _(0.1) | 4.2 _(0.2) | -34 ₍₁₎ | 14.6 | 32 |
| (15N)CH ₂ -CO-N(C ₁₀ H ₂₁) ₂ | 14.3 _(0.1) | 3.6 _(0.4) | -36 ₍₁₎ | 14.6 | 32 |
| (15N)CH ₂ -CO-NHC ₅ H ₁₁ | 13.4 _(0.3) | 7.2 _(0.9) | -21 ₍₄₎ | 13.2 | 5 |
| (15N)CH ₂ -CO-NHC ₁₀ H ₂₁ | 13.5 _(0.2) | 6.4 _(0.4) | -24 ₍₂₎ | 13.2 | 5 |
| (15N)CH ₂ -CO-OC ₁₀ H ₂₁ | 13.8 _(0.1) | 3.8 _(0.5) | -34 ₍₂₎ | 12.7 | -7 |
| (18N)CH ₂ -CO-N(C ₅ H ₁₁) ₂ | ^a | | | 11.7 ^{b,c} | -28 ^{b,c} |
| (18N)CH ₂ -CO-N(C ₁₀ H ₂₁) ₂ | | | | 11.9 ^{b,c} | -26 ^c |
| (18N)CH ₂ -CO-NHC ₁₀ H ₂₁ | | | | <11.5 ^{b,c} | <-40 ^{b,c} |
| (18N)CH ₂ -CO-NHC ₁₈ H ₃₇ | | | | <11.5 ^{b,c} | <-40 ^{b,c} |
| (15N)CH ₂ -CO-OC ₁₀ H ₂₁ | | | | <11.2 ^{b,c} | <-40 ^{b,c} |
| (18N)[CH ₂ -CO-N(C ₅ H ₁₁) ₂] ₂ | | | | 11.8 ^{b,c} | -28 ^{b,c} |

^a Cannot be determined in the available temperature range. ^b Measured at 2:1 L:Na⁺ ratio. ^c Measured at 1:1 L:Na⁺ ratio. ^d All data which are not labeled are measured at 1:1 L:Na⁺ ratio. The numbers in the parentheses are the standard deviations.

since solvation of cations in lipophilic membrane environments may be stabilized by such cooperative effects. This mechanism is determined exclusively by the nature of the sidearms connected to the macrocyclic polyether and seems to be insensitive to the nature of the macroring size itself.

It was possible to identify and quantify an additional kinetic process, which has been tentatively assigned to nitrogen inversion within the complexes. As expected, the 18-C-6 derivative complexes exhibited much lower barriers for this inversion than the corresponding 15-C-5 and 12-C-4 analogues. Interestingly, but perhaps not so surprisingly, it was observed that this nitrogen inversion process had approximately equal kinetic parameters as the cation exchange reaction for the 15-C-5 derivative series. This is indicative of more rigid complexes in this series when compared with the 18-C-6 analogues, where molecular motions are more intimately coupled.

Experimental Section

The syntheses, properties, and characterization of the aza-crown ether ligands used in the present study have been previously described in detail.^{5,21}

Sodium tetraphenylborate (NaBPh₄, Aldrich, Gold Label) was recrystallized from acetonitrile and vacuum dried at 40 °C for at least 24 h prior to use. Calcium perchlorate (Sigma) was vacuum dried at 60 °C for 24 h and weighed in a drybox and then dissolved in CD₃CN to prepare a concentrated stock solution. Calcium complexes were made by adding equivalent amounts of this stock solution into carefully prepared aza-crown ether ligand CD₃CN solutions. CD₃CN (Aldrich) was used directly as received.

All NMR measurements were carried out using a Varian VXR 400 spectrometer, operating at 399.852 MHz for ¹H. The

chemical shifts of the proton signals were referenced to the center peak of acetonitrile, at 1.930 ppm. Except for the variable temperature experiments, all spectra shown were acquired at a probe temperature of 294 ± 1 K. For the variable temperature experiments, sample temperature was controlled with a Varian VXR-400S variable temperature unit to within ±0.5 K. The temperature range was between 233 and 343 K. Sample concentrations were usually 10 mM for the ligands, unless otherwise specified. ¹H NMR spectra were recorded in 5-mm tubes.

¹H NMR spectra were typically acquired with 40K data points and zero-filled to 80K. COSY spectra were acquired in a 1K by 512 data matrix and zero-filled to 1K by 1K. Pulses (90°) of 32 μs, pulse delays of 1.0 s, and line broadening of 0.5 Hz were used for all experiments.

Activation enthalpies and entropies were calculated from the Eyring plots by using the program MINSQ. The errors on ΔH^{\ddagger} and ΔS^{\ddagger} are the standard deviations of the linear regressions of the Eyring plots. The standard deviations for $\Delta G^{\ddagger}_{21^{\circ}\text{C}}$ were calculated by using the approximate equation $\sigma(\Delta G^{\ddagger}) = |\sigma(\Delta H^{\ddagger}) - T\sigma(\Delta S^{\ddagger})|$.³⁰ For calculating $\Delta G^{\ddagger}_{\text{c}}$, $\delta\nu$ is the chemical shift difference at the extreme slow exchange condition. For those cases for which this condition could not be reached, the chemical shift difference between that of the pure ligand and that of its 1:1 complex at room temperature was used in the calculations.

Acknowledgment. The authors express their gratitude to the NIH (Grant GM-33940) and the NSF (Grant DMR-9119986) for partial support of this work. The authors also express their gratitude to Drs. Jeanette Hernández and George Gokel for supplying the ligands used in the present study.^{5,21}

(30) Binsch, G.; Kessler, H. *Angew. Chem., Int. Ed. Engl.* 1980, 19, 411.